Journal of Hazardous Materials 192 (2011) 160–167

Contents lists available at ScienceDirect

Journal of Hazardous Materials

journal homepage: www.elsevier.com/locate/jhazmat

Local characteristics of cross-unit contamination around high-rise building due to wind effect: Mean concentration and infection risk assessment

X.P. Liu[a,b], J.L. Niu[b,*], K.C.S. Kwok[c], J.H. Wang[d], B.Z. Li[d]

[a] State Key Laboratory of Fire Science, University of Science and Technology of China, Hefei 230027, PR China
[b] Department of Building Services Engineering, The Hong Kong Polytechnic University, Hong Kong
[c] CLP Power Wind/Wave Tunnel Facility, Hong Kong University of Science and Technology, Hong Kong
[d] Faculty of Urban Construction and Environmental Engineering,Chongqing University, Chongqing 400030, PR China

ARTICLE INFO

Article history:
Received 15 February 2011
Received in revised form 28 April 2011
Accepted 30 April 2011
Available online 11 May 2011

Keywords:
Hazardous gas dispersion
High-rise residential building
Wind tunnel
Infections risk assessment

ABSTRACT

In this present work, the characteristics of hazardous gas dispersion and possible cross-unit contamination around a complex-shaped high-rise residential building due to wind effect are thoroughly studied using physical modeling method. Experiments were performed in a boundary layer wind tunnel for a 1:30 scale model that represented a 10-story residential building in prototype. Tracer gas, simulating exhausted room air, was continuously released from different floor levels, and its concentrations on the adjacent envelope surfaces were measured using fast flame ionization detectors. The mean concentration fields were reported and analyzed under different configurations during the experiment to consider the effects on pollutant dispersion behavior due to changes in source position and approaching wind condition, with the main emphasis on the differences between open-window and closed-window conditions. In particular, the measured concentration fields were further examined from a practical point of view, with respect to hazard assessment. Understanding these hazardous plume dispersion features is useful for employing effective intervention strategies in modern residential building environment in case of hazardous substance release. The study on this physical process is not only helpful to reduce the hazardous effect of routine release of harmful pollutant near the building, but also useful for the purpose of prevention and control of accidental infectious diseases outbreak.

1. Introduction

Air pollution can have a wide range of negative consequences for public health. Understanding the characteristics of hazardous plume dispersion in typical building environment is the prerequisite for risk assessment. Many previous studies have been conducted on the behavior of plumes released near different urban environments, ranging from city scale [1], building arrays [2], street canyons [3] to an isolated single building [4]. A large body of work on pollutant dispersion in urban areas over different scales has been summarized by Britter and Hanna [5].

In recent years, the possible airborne transmission route of highly infectious diseases within building environment has attracted great attention. The infectious particles were often considered to be droplet nuclei, which can remain airborne for prolonged periods because of their low settling velocity. Infection via inhalation of pathogen-carrying droplet nuclei is termed "airborne transmission" [6]. It has been proved that many infections including tuberculosis (TB) [7], measles [8] and influenza [9] can be spread by the airborne route. In particular, Yu et al. [10] published the key findings in *the New England Journal of Medicine*, for the SARS outbreak in one real estate (Amoy Garden) in Hong Kong. Their epidemiologic analysis and experimental studies, supplemented with airflow simulations supported the probability of an airborne spread of the SARS virus in this large community outbreak. These increased concerns over the effects of pollution on human health and the requirements in preventing infectious disease transmission have also increased the need for thorough studies of pollutant dispersion around buildings, especially in high densely populated areas with crowd living conditions.

In many metropolitan areas, a large number of people live in high-rise residences. The changes in building design were devised to improve land use efficiency, but led to more complex dispersion routes of pollutant that have not been observed before [11]. Under crowd living conditions, the air pollutant exhausted from one household could probably re-enter into the neighboring households. Our previous works, applying both on-site measurement and numerical simulation methods [12–14], identified the possible vertical transmission path in high-rise residential (HRR) buildings with

* Corresponding author. Tel.: +852 2766 7781; fax: +852 2774 6146.
E-mail addresses: bejlniu@polyu.edu.hk, bejlniu@inet.polyu.edu.hk (J.L. Niu).

0304-3894/$ – see front matter © 2011 Elsevier B.V. All rights reserved.
doi:10.1016/j.jhazmat.2011.04.106

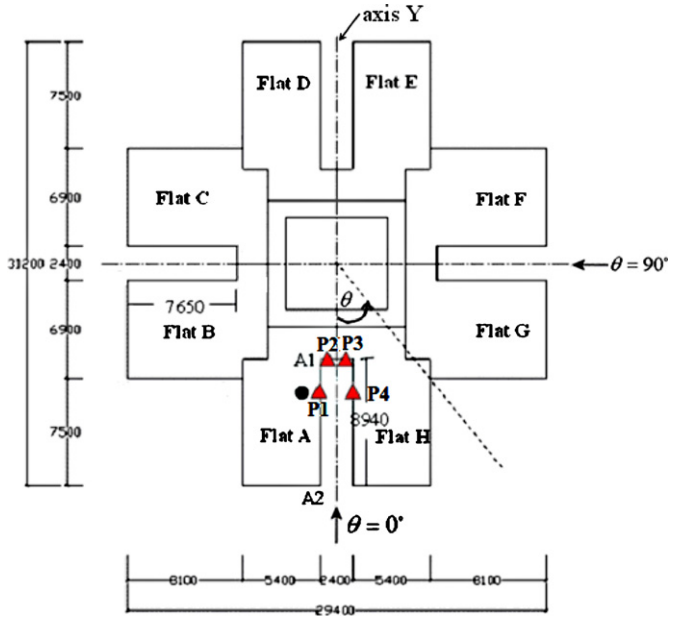

Fig. 1. Plan view of the building model (dimensions in mm) with the tracer gas source and measurement locations (source position: ●; measurement points: ▲).

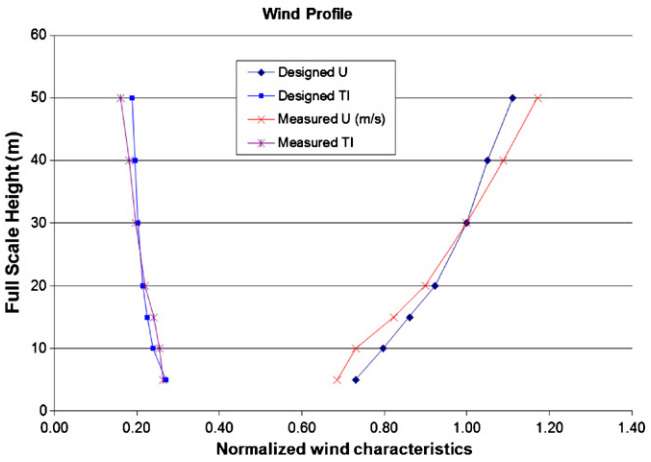

Fig. 2. Normalized wind profile of the approaching wind.

single-side open-window due to buoyancy effect. It was revealed that the room upstairs could contain up to 7% of the exhaust air from the immediately adjacent flat downstairs when the wind speed is relatively low, which led to a cross-contamination.

The objective of this study is to further investigate the wind-induced pollutant dispersion process around a typical HRR building in Hong Kong, with a complex building shape. The floor plan of the studied building is in cross shape #, and each floor contains eight units. The plan view of this kind of building is shown in Fig. 1. It comprises a central core and residential units extending outward from the core in eight directions, consequently four semi-closed, so-called re-entrant spaces are formed in each high-rise block. This design is to fulfill the relevant Building Regulations [15] and code of practice in force in Hong Kong. Then, each room in a unit may have more external wall and window areas, accessible to daylight and outside air. However, such building design can lead to the accumulation of pollutants and subsequent cross-contamination in the re-entrant space. A number of investigations of the re-entrant effects on the pollutant dispersion have been conducted [16,17]. In order to investigate the detailed mechanisms of such process, a series of experiments were designed and undertaken in a boundary layer wind tunnel. The cross-contamination has been preliminarily reported in our earlier paper, without considering the window's effect and the practical impact due to this phenomenon [18]. In this paper, the mean concentrations at different positions under both normal and oblique wind directions were measured and analyzed to reveal the detailed hazardous plume dispersion mechanisms under the effect of wind, with both closed-window and open-window conditions. For modern residential buildings, the indoor temperature is usually higher than outdoors due to insolation and the numbers of electronic devices even though they are not in use [19]. Under such circumstance, residents would be most likely to open the windows to provide cooling and ventilation, which can be reasonably expected to result in different dispersion features between different window configurations.

Moreover, the measured concentrations were further examined from the practical point of risk analysis. With regard to the airborne transmission risk of highly infectious diseases, one quantitative infection risk assessment model, i.e., the Wells–Riley model [8], was employed to evaluate the risk of these diseases to the neighbors based on the measured concentrations. This model has been widely used to estimate the infection risk in enclosed spaces [20], including hospital wards [21] and public transportation facilities [22]. In this study, the assessment was conducted based on both mean and the instantaneous peak concentration values. The results are compared to estimate the potential cross-unit contamination risks induced by either mean or instantaneous peak concentration presented during one inhalation period of humans.

2. Methodology

2.1. Experimental design

The experiments were undertaken in the low speed section of Wind/Wave Tunnel [23]. Roughness elements, spires and fences were used to generate the boundary layer flow in the wind tunnel with a power law profile having an exponent of 0.2. The turbulence intensity profile of the approaching wind flow was simulated in accordance with Terrain Category 2 stipulated in Australian/New Zealand Standard [24]. The mean velocity profile was presented by wind velocity ratio U_{VR} defined as $U(Z)/U_{Ref}$ to satisfy the boundary conditions similarity criteria. It was normalized by the appropriate characteristic velocity U_{Ref} which was selected as the wind velocity at building height in this experiment. The approach flow profiles [25] was measured 1.5 M upstream of the building model location. The designed and measured mean velocity and turbulence intensity profile were shown in Fig. 2.

For wind tunnel modeling of flow and plumes dispersion, one set of requirements for similarity between scale model and prototype should be carefully examined, which have been reported in several literature [26,27]. Within these similarity conditions, several of the dimensionless parameters can be neglected due to their low relative importance when simulating transport and dispersion around buildings, while Reynolds number (Re) independence is required in terms of the normalized Navier–Stokes equation. When the Reynolds number is sufficiently large, both flow and scalar dispersion are effectively independent of Re, without considering thermal effects. This has become a standard concept in wind tunnel modeling of dispersion [28]. It is now known that the criteria are affected by source location, building orientation, and measurement location [29]. Simulations for measurement locations in the middle to far wake region ($x > 1H$ downwind) may only require $Re = U_H H/\nu > 3000$ if a truly turbulent exhaust plume exists. How-

Table 1
Configuration of each case (closed-window).

Case no.	E1	E2	E3	E4	E5	E6	E7	E8	E9	E10	E11	E12
Source location	3rd Floor	6th Floor	9th Floor	3rd Floor	6th Floor	9th Floor	3rd Floor	6th Floor	9th Floor	3rd Floor	6th Floor	9th Floor
Orientation	$\theta = 0^\circ$	$\theta = 0^\circ$	$\theta = 0^\circ$	$\theta = 180^\circ$	$\theta = 180$	$\theta = 180$	$\theta = 45^\circ$	$\theta = 45^\circ$	$\theta = 45^\circ$	$\theta = 90^\circ$	$\theta = 90^\circ$	$\theta = 90^\circ$

ever, concentration distributions on the building surface itself may vary with wind speed until *Re* values exceed 15,000 [30], since the produced smaller plumes will be dominated more by plume size eddies rather than building size eddies, which is likely to make their dilution more Reynolds number dependent. With respect to our investigations, the approach velocity measured in the wind tunnel at building height (1 m at model scale) was 3.27 m/s, the Reynolds number of wind tunnel modeling is about 2×10^5 which is much larger than the criteria. Thus the Reynolds independence can be satisfied.

The sketch map of the experimental configuration was shown in Fig. 1. One 1:30 scale model was constructed to represent a 10 stories HRR building with 30 m height in prototype. Such a large-scale model can allow greater spatial resolution of concentration data [31], while the blockage ratio in the wind tunnel is controlled at approximately 5% to minimize the requirements for blockage correction [32]. In addition, the model does not exceed half the wind tunnel height during the experiments. In this study, we confined ourselves to a single, stand-alone building in order to simplify the problem, and the influence introduced by neighboring HRR building was ignored although majority of the Hong Kong buildings in reality are clustered. The wind direction was represented by θ, defined as the angle between the wind direction and the axis *Y* of symmetry of the building plan, as shown in Fig. 1. The tracer gas used is propane of 99,000 ppm concentration. The density difference between this tracer gas and air is within 5%, thus the buoyancy effect is negligible during this experiment. The tracer gas sources were located at three different floors in one of the re-entrant spaces, respectively at the 3rd floor, the 6th floor and the 9th floor on façade A1–A2. The tracer gas was released through a flow-meter at a constant flow rate (58.5 ml/s) at a nozzle exit, which was flush with the building surface. The exit opening was enlarged to make sure the velocity of the source gas was low to 0.38 m/s, which was about one order of magnitude lower than the wind speed. Thus it can be assumed that source momentum effects were not significant. The concentration measurements were taken on the building surfaces at four points each floor, as shown in Fig. 1.

As summarized in Table 1, a series of testing cases were first conducted with four wind directions under closed-window condition. After that, all the cases were repeated under open-window condition to evaluate the effect induced by the residents' behavior of window opening. In the building model, 4 of the 8 units (Flats A, B, H and G) in each floor have been designed to have openable windows with effective open area equal to 50% of the real window size. According to the relevant building regulations in Hong Kong [33], the window's area should be at least equal to 1/16th of the floor area of the room for the purpose of natural ventilation. Also, China Standard [34] specified that for each dwelling, the window's area should be no less than 1/20th of the floor area. Therefore, the window-to-floor area ratio for the present model is controlled at approximately 7.4%. The window's location and size were shown in Fig. 3, while the height of all the windows is 900 mm (in prototype). With the door of each unit closed, the external wind flow can only flow across the building model through the designed open-window located in the 4 units. The pollutant dispersion routes could be more complicated when all the units have open windows and doors, due to the internal cross ventilation through the corridors, and it is out of the scope of the present work.

2.2. Measurement method

Cobra probe was used to determine the wind profile due to its advantages and reliability [35], with an accuracy of ±0.3 m/s and ±1° pitch and yaw up to about 30% turbulence intensity. The detection of propane concentrations was achieved with a fast-response flame ionization detector (FID) model HFR400 [36]. Four FID sets were used to simultaneously sample the building surface concentrations. At each measurement position, sample air was collected via sampling tubes over a period of 120 s at a data-acquisition rate of 150 Hz to obtain stable estimates of mean concentration. The measurements correspond to full-scale concentrations obtained in a 1-h period. The signal was then passed through a low pass filter which effectively eliminates the alias errors, and was post-processed digitally to obtain the desired mean values, variances and related statistical quantities. For each stage of experiment, concentration measurements were taken at each floor at different facades within the re-entrant space to enable dispersion patterns to be mapped out in detail. The background concentration in the wind tunnel was measured upstream of the model and subtracted from the measured concentrations.

The calibration of the fast FID was carried out using synthetic air and certified calibration gases of different concentrations (from 51.2 ppm to 99,000 ppm). The calibration was repeated to ensure that the calibration error is generally within 10% when it was used to measure the standard gas with the lowest concentration, which is 51.2 ppm. It was also found that that there was considerable variation in the FID calibration from day to day, as reported by Baker and Hargreaves [37]. Thus the calibration was performed before and after each series of experiment to check the stability of the equipment.

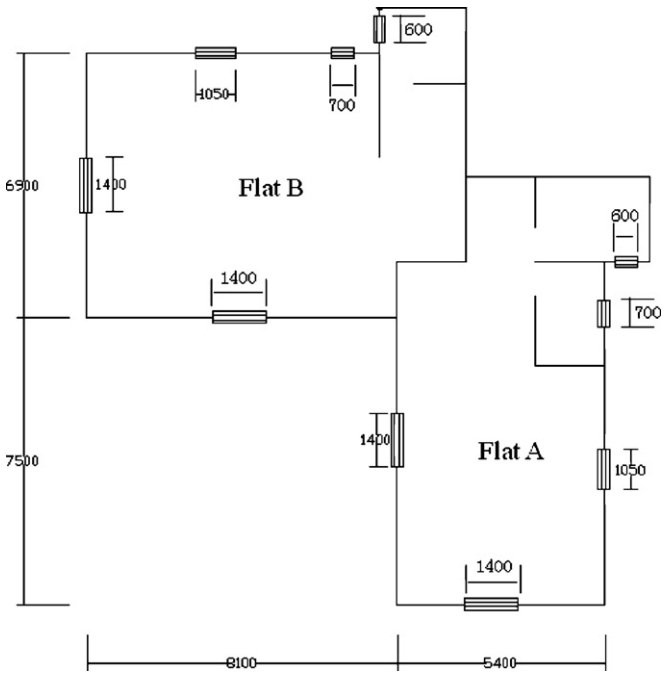

Fig. 3. Detailed window size and positions.

3. Results and discussions

3.1. Normalized mean concentration profiles

The normalized mean concentration profiles were presented using the usual form of non-dimensional concentration $K_c = C_{mean}U_H H^2/Q$ where C_{mean} is the measured mean concentration value, U_H is the mean wind speed at height H, H is the building height and Q is the volumetric flow rate of the gas source. The dimensionless concentration expresses the absolute differences of concentrations for different configurations under room temperature. The mean concentration distributions combined with surface pressure distributions under closed-window condition have been discussed before [18], thus the discussion presented here is mainly focused on the differences between open and closed-window conditions.

Figs. 4–6 show the normalized mean concentration coefficients at each floor under different wind directions, when the source was located in the 3rd, 6th and 9th floor, respectively. By examining the mean concentration values at different locations, the influenced regions under various kinds of configurations can be clearly seen from the results. Considering window's effect, it can be observed that the plume dispersion characteristics were similar under both window configurations, while the concentration level in each measurement point would be lowered when the windows were open. The variation trends of measured mean concentration were about the same under both window opening conditions. Both the vertical and horizontal dispersion reported by Liu et al. [18] under closed-window conditions can still be found from the results obtained under open-window conditions. The air pollutant exhausted from the index unit (Flat A) can be transported through the re-entrant space to the window's location of either Flat H in the horizontal direction, or to the other flats (Flats A and H) located in the vertical adjacent floors. The highest concentration presented in the source floor, and the concentrations at other floors generally decreased with distance from the source floor, both upward and downward in the vertical direction, while the concentration level reduced more rapidly under open-window conditions. It should also be noticed that the concentration detected at different facade in the same floor were considerably different under open-window condition, especially in the source floor, while it was close to each other under closed-window condition. Part of the tracer gas that penetrated indoors via the open windows contributed to the reduced concentration levels obtained at the window's locations. With regard to different source positions, it can be found that the open-window effect was more obvious when the source was located in the middle height of the building. For example, as shown in Fig. 5(a) and (c), the concentration values measured in two floors away from the source floor were clearly reduced with open-window condition, while the concentration level can be of the same magnitude as that of the source floor when the windows were closed.

With regard to different wind directions, when the wind incident angle were 0° and 180°, the largest discrepancy in concentration magnitude was found in case E2, as shown in Fig. 5(a), when the source was located in the 6th floor, the concentration values obtained in $\theta = 0°$ under closed-window condition were about 4

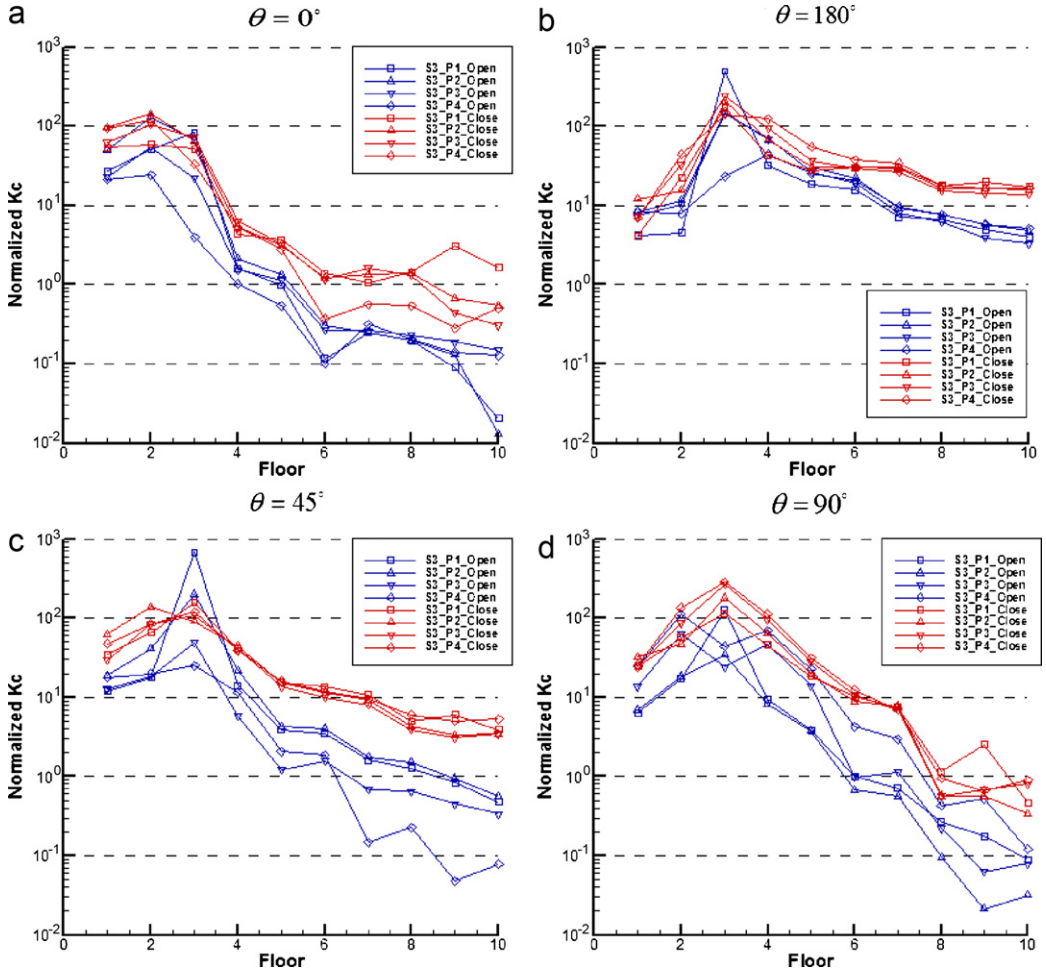

Fig. 4. (a–d) Normalized concentration distributions under different wind directions, when tracer released at the 3rd floor.

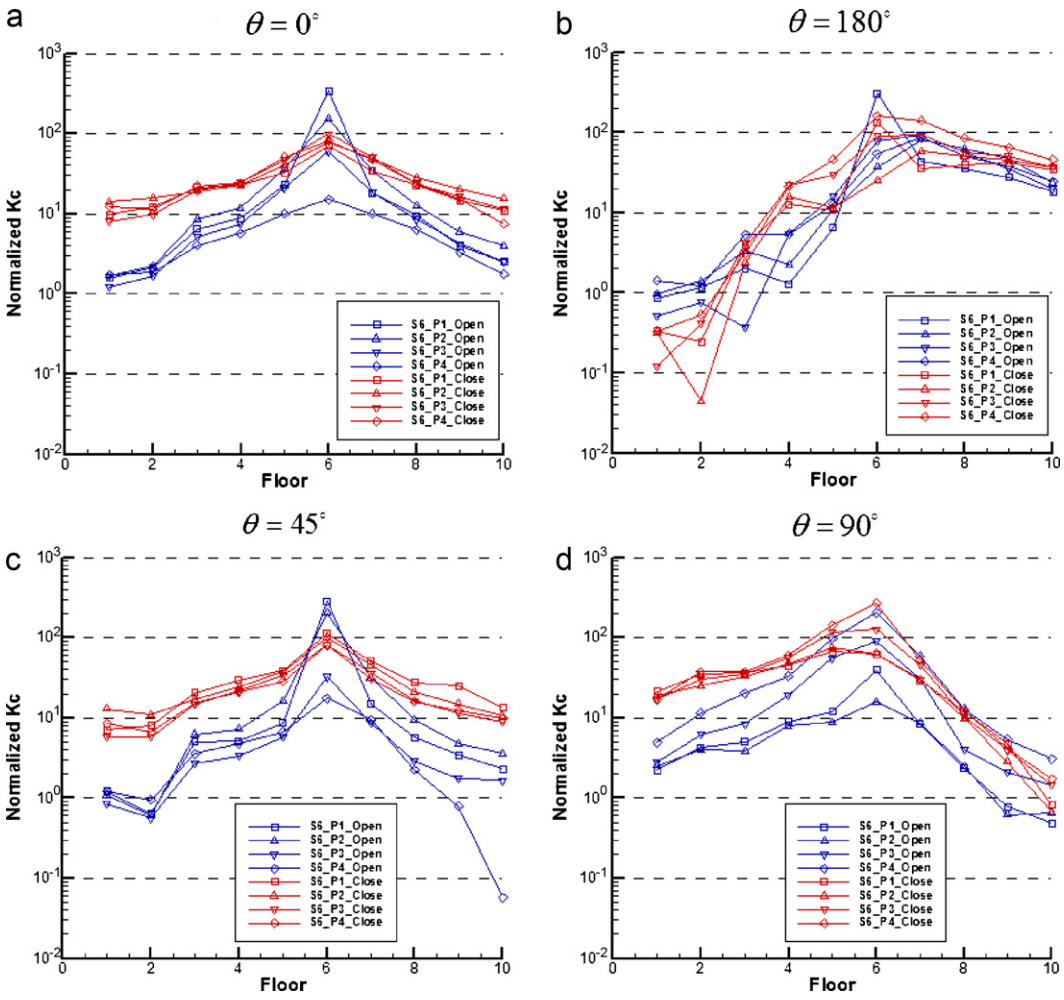

Fig. 5. (a–d) Normalized concentration distributions under different wind directions, when tracer released at the 6th floor.

times (measured by an average of all the measurements) larger than those obtained under open-window condition. When the wind incident angles were 45° and 90°, the overall concentration levels were obviously lower when there are openings along building facades. The dilution effect induced by cross-ventilation under these two wind directions is relatively stronger than that under the other two wind directions. With open windows, the airflow across the building wings can effectively increase the air change rate in the re-entrant space, in contrast to the "air curtain" effect across the opening of the re-entrant space under closed-window condition. Taking no account of the extremely low concentration values, for each pair of cases with the same wind direction and the source location, the averaged $K_c(close)/K_c(open)$ ratio were from 4 to 7. For each individual measurement point, the ratio is ranged from about 1 to 12.

It can be concluded that under the current configurations, when the window-to-floor area ratio is approximately 7.4%, the key features of wind-induced near-building dispersion are similar between open-window and closed-window situations. The obvious differences of mean concentration profiles only exist in the concentration magnitudes, the concentrations measured under open-window condition are generally within one order of magnitude less than those under closed-window conditions.

3.2. Infection risk assessment

Based on the concept of "quantum of infection" (a quantum is defined as the number of infectious airborne particles required to infect the person and may consist of one or more airborne particles), the Wells–Riley equation is presented for the purpose of estimating the probability of airborne transmission of an infectious disease [8]

$$P = \frac{C}{S} = 1 - \exp\left(-\frac{Iqpt}{Q}\right) \quad (1)$$

where p is the probability of infection, C is the number of infection cases, S is the number of susceptibles, I is the number of infectors, P is the pulmonary ventilation rate of a person, q is the quanta generation rate, t is the exposure time interval, and Q is the room ventilation rate. The Wells–Riley equation is set up on the assumptions of a well-mixed and steady-state condition. However, the equation can also incorporate spatially distributed infection risk by conducting tracer gas measurements, which does not require the assumptions [38]. Some risk assessment studies have also used these approaches to estimate the infection risk, by employing numerical simulation method [13,21]. Here using the experimental results, the infection risk of highly infectious diseases such as measles can be evaluated.

ASHRAE [39] recommends that residential buildings taller than three stories would require an amount of fresh air intake of 0.03 l/s m^2, which is assumed as the constant room ventilation rate during the following studies. Supposing a hypothetical measles outbreak with a high values for quantum generation rate at the source location, $q = 570\ h^{-1}$ [40], pulmonary ventilation rate at 0.6 m^3/h [13], the calculated infection probabilities are listed in Table 2. The corresponding exposure time is 1 h. The following results were cal-

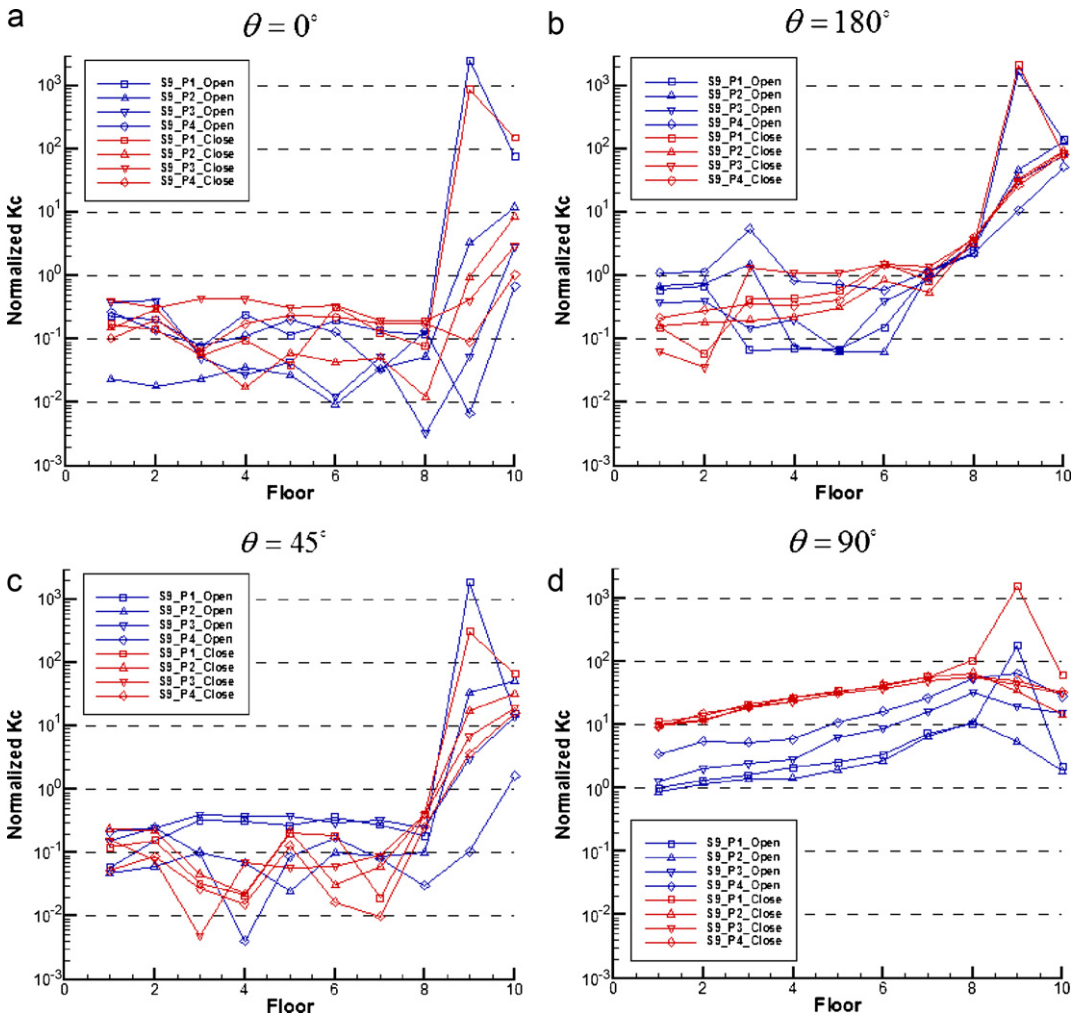

Fig. 6. (a–d) Normalized concentration distributions under different wind directions, when tracer released at the 9th floor.

culated by the data obtained under closed-window condition when the source was located in the 6th floor, considering its relatively high mean concentrations obtained under this configuration. These results give an estimation of the infection risk level at different positions. In general, the infection risk can remain in a non-negligible level even at several floors away from the source location under different conditions. In particular, the probabilities can be greater than 10% in vertical adjacent flats and the opposite flat when $\theta = 45^\circ$ and $\theta = 90^\circ$. The highest infection risk can be up to 23%, in the opposite flat when $\theta = 90^\circ$, indicating that the hazardous plume can be accumulated in the deep side of the re-entrant space and lead to a high infection risk. These mean infection risk probabilities show that in case of an outbreak of highly infectious disease, both the vertical and horizontal transports of infectious diseases in high-rise residential buildings are worthy of due consideration in infection control. And the spatial distribution of infection risk can be characterized by the mean concentration distributions.

Moreover, it was noticed during the experiment that the transient concentrations can be significantly higher than the mean concentrations. For the prevention of highly infectious disease, it is necessary to check the practical impacted induced by the instantaneous peak concentrations. The instantaneous concentrations should be analyzed with a time scale as small as one inhalation period of humans (between 1 and 2 s). As for this aspect, the original data-acquisition frequency of 150 Hz is not required. Thus, all the instantaneous concentration values were calculated using the 2 s-averaged (in prototype) data, and the corresponding infection risks calculated by peak concentration values were shown in Table 3.

Table 2
Infection risks calculated by mean concentration values (source located in the 6th floor with closed windows).

	$\theta = 0^\circ$				$\theta = 180^\circ$				$\theta = 45^\circ$				$\theta = 90^\circ$			
Floor	P1	P2	P3	P4	P1	P2	P3	P4	P1	P2	P3	P4	P1	P2	P3	P4
3	2.06	1.86	1.87	2.13	0.37	0.23	0.40	0.30	1.98	1.65	1.44	1.49	3.46	3.17	3.40	3.59
4	2.21	2.18	2.35	2.35	1.21	1.51	2.12	2.05	2.83	2.31	2.10	2.01	4.27	4.51	5.32	5.68
5	3.11	3.86	4.52	4.80	1.04	1.11	2.84	4.35	3.71	3.58	3.28	2.75	6.24	7.06	10.70	13.07
6	6.59	7.39	9.14	7.60	12.09	2.39	8.42	14.24	10.47	9.35	7.55	7.54	5.90	5.99	11.65	23.06
7	3.25	4.63	4.76	4.48	3.37	5.47	8.54	12.77	4.87	4.33	3.44	2.94	2.79	2.86	4.31	5.05
8	2.16	2.67	2.29	2.26	3.77	4.79	5.35	7.87	2.63	2.01	1.56	1.54	1.15	0.94	1.01	1.17
9	1.41	1.95	1.58	1.48	3.98	4.36	4.77	6.09	2.41	1.44	1.12	1.19	0.46	0.28	0.38	0.40

Table 3
Infection risks calculated by instantaneous peak concentration values (source located in the 6th floor with closed windows).

	$\theta = 0^\circ$				$\theta = 180^\circ$				$\theta = 45^\circ$				$\theta = 90^\circ$			
Floor	P1	P2	P3	P4	P1	P2	P3	P4	P1	P2	P3	P4	P1	P2	P3	P4
3	0.01	0.01	0.01	0.01	0.01	0.00	0.01	0.01	0.01	0.01	0.01	0.01	0.01	0.01	0.01	0.01
4	0.01	0.01	0.02	0.01	0.01	0.01	0.02	0.02	0.01	0.01	0.01	0.01	0.01	0.01	0.02	0.02
5	0.02	0.02	0.03	0.03	0.01	0.02	0.03	0.03	0.02	0.02	0.02	0.02	0.02	0.02	0.03	0.03
6	0.03	0.03	0.03	0.04	0.05	0.03	0.03	0.03	0.04	0.03	0.03	0.03	0.03	0.03	0.04	0.06
7	0.02	0.02	0.02	0.03	0.01	0.02	0.03	0.03	0.02	0.02	0.02	0.02	0.02	0.02	0.03	0.03
8	0.01	0.01	0.01	0.02	0.01	0.01	0.02	0.02	0.01	0.01	0.01	0.01	0.02	0.01	0.01	0.02
9	0.01	0.01	0.01	0.01	0.02	0.01	0.01	0.01	0.01	0.01	0.01	0.01	0.01	0.01	0.01	0.01

It can be seen that the probability calculated by instantaneous peak concentration values is under 0.06% in all the positions for the presented cases. This suggests that the infection risk caused by a transient peak concentration level that is detected in a short time duration can be neglected, comparing with mean infection risk probabilities. Although the peak concentration value can be clearly higher than the mean value, the risk is still significantly low due to the extremely short exposure time. The spatial distribution of infection risk is still characterized by the mean concentration distribution.

4. Conclusions

In the present paper, the time-averaged characteristics of hazardous gas dispersion around a complex-shaped high rise building due to wind effect were thoroughly investigated in a wind tunnel study. Such dispersion process is found to be much more complicated than that of under buoyancy effect. The experimental results illustrate that the flow pattern around the HRR building has the potential to transport gaseous pollutant within the re-entrant space under both open-window and closed-window conditions. The influenced region, the dispersion route, the strength of contaminant concentration and its exposure risks due to this kind of dispersion are investigated in this study.

The mean concentrations at different locations was measured to illustrate the dispersion route and get valuable information about hazardous gas dispersion around one typical HRR building, with the main emphasis on the comparisons between different window opening conditions. The mean concentration distributions under both configurations were found to be similar. Both the vertical and horizontal dispersion revealed by Liu et al. [18] under closed-window condition can still be found when the windows are open. The obvious differences of mean concentration profiles only exist in the concentration magnitudes, the overall concentration level is clearly reduced under open-window condition, especially when the approaching wind incident angle are 45° and 90°. This implies that, when the windows are open, the tracer gas is not only restricted in the re-entrant space, but can penetrate indoors through the open-windows, which results in the decreased concentration level detected at the windows' location. Furthermore, a widely used infection risk assessment model was employed to examine the potential risk in case of an outbreak of highly infectious disease, in terms of both mean and the instantaneous peak concentrations. The spatial distribution of infection probabilities shows that the risk of airborne transmission in neighboring households are not negligible, and can be up to 20% in particular position, which should be paid attention to in terms of infection control. Moreover, a transient peak concentration level that is detected in a short time duration can be neglected, comparing with mean infection risk probabilities. The spatial distribution of infection risk is still characterized by the mean concentration distribution. However, it should be noted that under some certain circumstances such as household flammable gas leakage, the unsteady characteristics of this dispersion process should not be overlooked, and the peak concentrations should be taken into considerations.

Understanding these pollutant transmission paths is useful in employing effective intervention strategies for pollution control in modern residential building environment. The study on this physical process is not only helpful to reduce the hazardous effect of routine release of harmful pollutant near the building, but also useful for the purpose of prevention and control of accidental infectious diseases outbreak. Based on the obtained results and the risk estimations, it is hoped that the corresponding strategies and optimization plan can be established. Also, the present studies were focused on wind-induced cross-unit contamination, without considering indoor–outdoor temperature differences. The dispersion characteristics under combined effect of wind and buoyancy could be more complicated and deserve further investigations.

Acknowledgements

The authors would like to thank Dr. Peter A. Hitchcock and his technical staff of CLP Wind tunnel, Hong Kong University of Science and Technology in preparing the scaled models and assisting the wind tunnel tests. The project is partially funded by Dean's Research funding FCLU, PolyU.

References

[1] M. Pontiggia, M. Derudi, M. Alba, M. Scaioni, R. Rota, Hazardous gas releases in urban areas: assessment of consequences through CFD modelling, J. Hazard. Mater. 176 (2010) 589–596.
[2] R.W. Macdonald, R.F. Griffiths, S.C. Cheah, Field experiments of dispersion through regular arrays of cubic structures, Atmos. Environ. 31 (1997) 783–795.
[3] S. Vardoulakis, B.E.A. Fisher, K. Pericleous, N. Gonzalez-Flesca, Modelling air quality in street canyons: a review, Atmos. Environ. 37 (2003) 155–182.
[4] I. Mavroidis, R.F. Griffiths, D.J. Hall, Field and wind tunnel investigations of plume dispersion around single surface obstacles, Atmos. Environ. 37 (2003) 2903–2918.
[5] S. Britter, S. Hanna, Flow and dispersion in urban areas, Annu. Rev. Fluid Mech. 35 (2003) 469–496.
[6] M. Nicas, W.W. Nazaroff, A. Hubbard, Toward understanding the risk of secondary airborne infection: emission of respirable pathogens, J. Occup. Environ. Hyg. 2 (2005) 143–154.
[7] E.A. Nardell, J. Keegan, S.A. Cheney, S.C. Etkind, Airborne infection. Theoretical limits of protection achievable by building ventilation, Am. Rev. Respir. Dis. 144 (1991) 302–306.
[8] E.C. Riley, G. Murphy, R.L. Riley, Airborne spread of measles in a suburban elementary school, Am. J. Epidemiol. 107 (1978) 421–432.
[9] R. Tellier, Review of aerosol transmission of influenza A virus, Emerg. Infect. Dis. 12 (2006) 1657–1662.
[10] I.T.S. Yu, Y. Li, T.W. Wong, W. Tam, A.T. Chan, J.H.W. Lee, et al., Evidence of airborne transmission of the severe acute respiratory syndrome virus, N. Engl. J. Med. 350 (2004) 1731–1739.
[11] J.L. Niu, Some significant environmental issues in high-rise residential building design in urban area, Energy Build. 36 (2004) 1259–1263.
[12] J.L. Niu, T.C.W. Tung, On-site quantification of re-entry ratio of ventilation exhausts in multi-family residential buildings and implications, Indoor Air 18 (2008) 12–26.
[13] N.P. Gao, J.L. Niu, M. Perino, P. Heiselberg, The airborne transmission of infection between flats in high-rise residential buildings: tracer gas simulation, Build. Environ. 43 (2008) 1805–1817.
[14] X.P. Liu, J.L. Niu, M. Perino, P. Heiselberg, Numerical simulation of inter-flat air cross-contamination under the condition of single-sided natural ventilation, J. Build. Perform. Simul. 1 (2008) 133–147.

[15] Building (Planning) Regulations, Laws of Hong Kong, Regulation 30: Lighting and ventilation of rooms used or intended to be used for habitation or as an office or kitchen; Regulation 31: Minimum requirements of window, The Hong Kong SAR Government, HK, 1984 (Chapter 123).
[16] Y. Li, S. Duan, I.T.S. Yu, T.W. Wong, Multi-zone modeling of probable SARS virus transmission by airflow between flats in Block E, Amoy Gardens, Indoor Air 15 (2004) 96–111.
[17] C.K.C. Cheng, K.M. Lam, Y.T.A. Leung, K. Yang, H.W. Danny Li, C.P. Sherman Cheung, Wind-induced natural ventilation of re-entrant bays in a high-rise building, J. Wind Eng. Ind. Aerodyn. 99 (2011) 79–90.
[18] X.P. Liu, J.L. Niu, K.C.S. Kwok, J.H. Wang, B.Z. Li, Investigation of indoor air pollutant dispersion and cross-contamination around a typical high-rise residential building: wind tunnel tests, Build. Environ. 45 (2010) 1769–1778.
[19] P.F. Linden, The fluid mechanics of natural ventilation, Annu. Rev. Fluid Mech. 31 (1999) 201–238.
[20] C.J. Noakes, C.B. Beggs, P.A. Sleigh, K.G. Kerr, Modelling the transmission of airborne infections in enclosed spaces, Epidemiol. Infect. 134 (2006) 1082–1091.
[21] H. Qian, Y. Li, P.V. Nielsen, X. Huang, Spatial distribution of infection risk of SARS transmission in a hospital ward, Build. Environ. 44 (2009) 1651–1658.
[22] H. Furuya, Risk of transmission of airborne infection during train commute based on mathematical model, Environ. Health Prev. Med. 12 (2007) 78–83.
[23] Experimental site wind availability data for central waterfront, Investigation Report WWTF007-2006, Planning Department, The Government of the Hong Kong Special Administrative Region.
[24] Australian Standard, Minimum Design Loads on Structures, AS1170.2-1989, 1989.
[25] B. Blocken, T. Stathopoulos, J. Carmeliet, Wind environmental conditions in passages between two long narrow perpendicular buildings, J. Aerospace Eng.-ASCE 21 (4) (2008) 280–287.
[26] J.E. Cermak, Physical modeling of flow and dispersion over complex terrain, Bound.-Layer Meteorol. 30 (1984) 261–292.
[27] K. Uehara, S. Wakamatsu, R. Ooka, Studies on critical Reynolds number indices for wind-tunnel experiments on flow within urban areas, Bound.-Layer Meteorol. 107 (2003) 353–370.
[28] W.H. Snyder, Guidelines for Fluid Modeling of Atmospheric Diffusion, EPA-600/8-81-009, National Technical Information Service, Springfield, VA, 1981.
[29] R.N. Meroney, Wind tunnel and numerical simulation of pollution dispersion: a hybrid approach, Invited Lecture, Croucher Advanced Study Insitute on Wind Tunnel Modeling, Hong Kong University of Science and Technology, 2004.
[30] N. Isyumov (Ed.), Dispersion Around Buildings, Chapter C7 of Wind Tunnel Studies of Buildings and Structures, ASCE Manuals and Reports on Engineering Practice No. 67, American Society of Civil Engineers, Reston, VA, 1999, pp. 137–142.
[31] P.J. Saathof, T. Stathopoulos, M. Dobrescu, Effects of model scale in estimating pollutant dispersion near buildings, J. Wind Eng. Ind. Aerodyn. 54–55 (1995) 549–559.
[32] J.B. Barlow, W.H. Rae, A. Pope, Low-speed Wind Tunnel Testing. (Third Edition), Wiley, New York, 1999.
[33] Building (Planning) Regulations, Laws of Hong Kong, The Hong Kong SAR Government, HK, 1997 (Chapter 123F).
[34] GB50368-2005, Residential building code, National standard, Complied by Ministry of Construction, PRC, 2005.
[35] S. Watkins, J. Milbank, B.J. Loxton, W.H. Melbourne, Atmospheric winds and their implications for microair vehicles, AIAA J. 44 (2006) 2591–2600.
[36] M. Pavageau, M. Schatzman, Wind tunnel measurements of concentration fluctuations in an urban street canyon, Atmos. Environ. 33 (1999) 3961–3971.
[37] C.J. Baker, D.M. Hargreaves, Wind tunnel evaluation of a vehicle pollution dispersion model, J. Wind Eng. Ind. Aerodyn. 89 (2001) 187–200.
[38] G.N. Sze To, C.Y.H. Chao, Review and comparison between the Wells–Riley and dose–response approaches to risk assessment of infectious respiratory diseases, Indoor Air 20 (2010) 2–16.
[39] American Society of Heating, Refrigerating and Air-conditioning Engineers, ASHRAE Standard 62-2007, Ventilation for Acceptable Indoor Air Quality, 2007.
[40] S.N. Rudnick, D.K. Milton, Risk of indoor airborne infection transmission estimated from carbon dioxide concentration, Indoor Air 13 (2003) 237–245.